

Studies of CP violation in $B^0 \rightarrow J/\psi K^{*0}$ decays

K. Abe,¹⁰ K. Abe,⁴⁶ N. Abe,⁴⁹ I. Adachi,¹⁰ H. Aihara,⁴⁸ M. Akatsu,²⁴ Y. Asano,⁵³
T. Aso,⁵² V. Aulchenko,² T. Aushev,¹⁴ T. Aziz,⁴⁴ S. Bahinipati,⁶ A. M. Bakich,⁴³
Y. Ban,³⁶ M. Barbero,⁹ A. Bay,²⁰ I. Bedny,² U. Bitenc,¹⁵ I. Bizjak,¹⁵ S. Blyth,²⁹
A. Bondar,² A. Bozek,³⁰ M. Bračko,^{22,15} J. Brodzicka,³⁰ T. E. Browder,⁹ M.-C. Chang,²⁹
P. Chang,²⁹ Y. Chao,²⁹ A. Chen,²⁶ K.-F. Chen,²⁹ W. T. Chen,²⁶ B. G. Cheon,⁴
R. Chistov,¹⁴ S.-K. Choi,⁸ Y. Choi,⁴² Y. K. Choi,⁴² A. Chuvikov,³⁷ S. Cole,⁴³
M. Danilov,¹⁴ M. Dash,⁵⁵ L. Y. Dong,¹² R. Dowd,²³ J. Dragic,²³ A. Drutskoy,⁶
S. Eidelman,² Y. Enari,²⁴ D. Epifanov,² C. W. Everton,²³ F. Fang,⁹ S. Fratina,¹⁵
H. Fujii,¹⁰ N. Gabyshev,² A. Garmash,³⁷ T. Gershon,¹⁰ A. Go,²⁶ G. Gokhroo,⁴⁴
B. Golob,^{21,15} M. Grosse Perdekamp,³⁸ H. Guler,⁹ J. Haba,¹⁰ F. Handa,⁴⁷ K. Hara,¹⁰
T. Hara,³⁴ N. C. Hastings,¹⁰ K. Hasuko,³⁸ K. Hayasaka,²⁴ H. Hayashii,²⁵ M. Hazumi,¹⁰
E. M. Heenan,²³ I. Higuchi,⁴⁷ T. Higuchi,¹⁰ L. Hinz,²⁰ T. Hojo,³⁴ T. Hokuue,²⁴
Y. Hoshi,⁴⁶ K. Hoshina,⁵¹ S. Hou,²⁶ W.-S. Hou,²⁹ Y. B. Hsiung,²⁹ H.-C. Huang,²⁹
T. Igaki,²⁴ Y. Igarashi,¹⁰ T. Iijima,²⁴ A. Imoto,²⁵ K. Inami,²⁴ A. Ishikawa,¹⁰ H. Ishino,⁴⁹
K. Itoh,⁴⁸ R. Itoh,¹⁰ M. Iwamoto,³ M. Iwasaki,⁴⁸ Y. Iwasaki,¹⁰ R. Kagan,¹⁴ H. Kakuno,⁴⁸
J. H. Kang,⁵⁶ J. S. Kang,¹⁷ P. Kapusta,³⁰ S. U. Kataoka,²⁵ N. Katayama,¹⁰ H. Kawai,³
H. Kawai,⁴⁸ Y. Kawakami,²⁴ N. Kawamura,¹ T. Kawasaki,³² N. Kent,⁹ H. R. Khan,⁴⁹
A. Kibayashi,⁴⁹ H. Kichimi,¹⁰ H. J. Kim,¹⁹ H. O. Kim,⁴² Hyunwoo Kim,¹⁷ J. H. Kim,⁴²
S. K. Kim,⁴¹ T. H. Kim,⁵⁶ K. Kinoshita,⁶ P. Koppenburg,¹⁰ S. Korpar,^{22,15} P. Krizan,^{21,15}
P. Krokovny,² R. Kulasiri,⁶ C. C. Kuo,²⁶ H. Kurashiro,⁴⁹ E. Kurihara,³ A. Kusaka,⁴⁸
A. Kuzmin,² Y.-J. Kwon,⁵⁶ J. S. Lange,⁷ G. Leder,¹³ S. E. Lee,⁴¹ S. H. Lee,⁴¹
Y.-J. Lee,²⁹ T. Lesiak,³⁰ J. Li,⁴⁰ A. Limosani,²³ S.-W. Lin,²⁹ D. Liventsev,¹⁴
J. MacNaughton,¹³ G. Majumder,⁴⁴ F. Mandl,¹³ D. Marlow,³⁷ T. Matsuishi,²⁴
H. Matsumoto,³² S. Matsumoto,⁵ T. Matsumoto,⁵⁰ A. Matyja,³⁰ Y. Mikami,⁴⁷
W. Mitaroff,¹³ K. Miyabayashi,²⁵ Y. Miyabayashi,²⁴ H. Miyake,³⁴ H. Miyata,³² R. Mizuk,¹⁴
D. Mohapatra,⁵⁵ G. R. Moloney,²³ G. F. Moorhead,²³ T. Mori,⁴⁹ A. Murakami,³⁹
T. Nagamine,⁴⁷ Y. Nagasaka,¹¹ T. Nakadaira,⁴⁸ I. Nakamura,¹⁰ E. Nakano,³³ M. Nakao,¹⁰
H. Nakazawa,¹⁰ Z. Natkaniec,³⁰ K. Neichi,⁴⁶ S. Nishida,¹⁰ O. Nitoh,⁵¹ S. Noguchi,²⁵
T. Nozaki,¹⁰ A. Ogawa,³⁸ S. Ogawa,⁴⁵ T. Ohshima,²⁴ T. Okabe,²⁴ S. Okuno,¹⁶
S. L. Olsen,⁹ Y. Onuki,³² W. Ostrowicz,³⁰ H. Ozaki,¹⁰ P. Pakhlov,¹⁴ H. Palka,³⁰
C. W. Park,⁴² H. Park,¹⁹ K. S. Park,⁴² N. Parslow,⁴³ L. S. Peak,⁴³ M. Pernicka,¹³
J.-P. Perroud,²⁰ M. Peters,⁹ L. E. Piilonen,⁵⁵ A. Poluektov,² F. J. Ronga,¹⁰ N. Root,²
M. Rozanska,³⁰ H. Sagawa,¹⁰ M. Saigo,⁴⁷ S. Saitoh,¹⁰ Y. Sakai,¹⁰ H. Sakamoto,¹⁸
T. R. Sarangi,¹⁰ M. Satapathy,⁵⁴ N. Sato,²⁴ O. Schneider,²⁰ J. Schümann,²⁹ C. Schwanda,¹³
A. J. Schwartz,⁶ T. Seki,⁵⁰ S. Semenov,¹⁴ K. Senyo,²⁴ Y. Settai,⁵ R. Seuster,⁹
M. E. Sevier,²³ T. Shibata,³² H. Shibuya,⁴⁵ B. Shwartz,² V. Sidorov,² V. Siegle,³⁸
J. B. Singh,³⁵ A. Somov,⁶ N. Soni,³⁵ R. Stamen,¹⁰ S. Stanič,^{53,*} M. Starič,¹⁵ A. Sugi,²⁴
A. Sugiyama,³⁹ K. Sumisawa,³⁴ T. Sumiyoshi,⁵⁰ S. Suzuki,³⁹ S. Y. Suzuki,¹⁰ O. Tajima,¹⁰
F. Takasaki,¹⁰ K. Tamai,¹⁰ N. Tamura,³² K. Tanabe,⁴⁸ M. Tanaka,¹⁰ G. N. Taylor,²³
Y. Teramoto,³³ X. C. Tian,³⁶ S. Tokuda,²⁴ S. N. Tovey,²³ K. Trabelsi,⁹ T. Tsuboyama,¹⁰

T. Tsukamoto,¹⁰ K. Uchida,⁹ S. Uehara,¹⁰ T. Uglov,¹⁴ K. Ueno,²⁹ Y. Unno,³ S. Uno,¹⁰
Y. Ushiroda,¹⁰ G. Varner,⁹ K. E. Varvell,⁴³ S. Villa,²⁰ C. C. Wang,²⁹ C. H. Wang,²⁸
J. G. Wang,⁵⁵ M.-Z. Wang,²⁹ M. Watanabe,³² Y. Watanabe,⁴⁹ L. Widhalm,¹³
Q. L. Xie,¹² B. D. Yabsley,⁵⁵ A. Yamaguchi,⁴⁷ H. Yamamoto,⁴⁷ S. Yamamoto,⁵⁰
T. Yamanaka,³⁴ Y. Yamashita,³¹ M. Yamauchi,¹⁰ Heyoung Yang,⁴¹ P. Yeh,²⁹ J. Ying,³⁶
K. Yoshida,²⁴ Y. Yuan,¹² Y. Yusa,⁴⁷ H. Yuta,¹ S. L. Zang,¹² C. C. Zhang,¹² J. Zhang,¹⁰
L. M. Zhang,⁴⁰ Z. P. Zhang,⁴⁰ V. Zhilich,² T. Ziegler,³⁷ D. Žontar,^{21,15} and D. Zürcher²⁰

(The Belle Collaboration)

¹*Aomori University, Aomori*

²*Budker Institute of Nuclear Physics, Novosibirsk*

³*Chiba University, Chiba*

⁴*Chonnam National University, Kwangju*

⁵*Chuo University, Tokyo*

⁶*University of Cincinnati, Cincinnati, Ohio 45221*

⁷*University of Frankfurt, Frankfurt*

⁸*Gyeongsang National University, Chinju*

⁹*University of Hawaii, Honolulu, Hawaii 96822*

¹⁰*High Energy Accelerator Research Organization (KEK), Tsukuba*

¹¹*Hiroshima Institute of Technology, Hiroshima*

¹²*Institute of High Energy Physics,*

Chinese Academy of Sciences, Beijing

¹³*Institute of High Energy Physics, Vienna*

¹⁴*Institute for Theoretical and Experimental Physics, Moscow*

¹⁵*J. Stefan Institute, Ljubljana*

¹⁶*Kanagawa University, Yokohama*

¹⁷*Korea University, Seoul*

¹⁸*Kyoto University, Kyoto*

¹⁹*Kyungpook National University, Taegu*

²⁰*Swiss Federal Institute of Technology of Lausanne, EPFL, Lausanne*

²¹*University of Ljubljana, Ljubljana*

²²*University of Maribor, Maribor*

²³*University of Melbourne, Victoria*

²⁴*Nagoya University, Nagoya*

²⁵*Nara Women's University, Nara*

²⁶*National Central University, Chung-li*

²⁷*National Kaohsiung Normal University, Kaohsiung*

²⁸*National United University, Miao Li*

²⁹*Department of Physics, National Taiwan University, Taipei*

³⁰*H. Niewodniczanski Institute of Nuclear Physics, Krakow*

³¹*Nihon Dental College, Niigata*

³²*Niigata University, Niigata*

³³*Osaka City University, Osaka*

³⁴*Osaka University, Osaka*

³⁵*Panjab University, Chandigarh*

³⁶*Peking University, Beijing*

³⁷*Princeton University, Princeton, New Jersey 08545*

³⁸*RIKEN BNL Research Center, Upton, New York 11973*

³⁹*Saga University, Saga*

⁴⁰*University of Science and Technology of China, Hefei*

⁴¹*Seoul National University, Seoul*

⁴²*Sungkyunkwan University, Suwon*

⁴³*University of Sydney, Sydney NSW*

⁴⁴*Tata Institute of Fundamental Research, Bombay*

⁴⁵*Toho University, Funabashi*

⁴⁶*Tohoku Gakuin University, Tagajo*

⁴⁷*Tohoku University, Sendai*

⁴⁸*Department of Physics, University of Tokyo, Tokyo*

⁴⁹*Tokyo Institute of Technology, Tokyo*

⁵⁰*Tokyo Metropolitan University, Tokyo*

⁵¹*Tokyo University of Agriculture and Technology, Tokyo*

⁵²*Toyama National College of Maritime Technology, Toyama*

⁵³*University of Tsukuba, Tsukuba*

⁵⁴*Utkal University, Bhubaneswar*

⁵⁵*Virginia Polytechnic Institute and State University, Blacksburg, Virginia 24061*

⁵⁶*Yonsei University, Seoul*

Abstract

An angular analysis for B decays into two vector mesons gives parameters sensitive to new physics. They are the decay amplitudes of the three helicity states, the asymmetry in triple product, and the CP violating phase. The measurements of these quantities are performed for $B^0 \rightarrow J/\psi K^{*0}$ decays in a data sample with 253 fb^{-1} taken by the Belle detector in the KEKB asymmetric e^+e^- collider. With the time-integrated angular analysis, the decay amplitudes' moduli and phase angles are measured to be $|A_0|^2 = 0.585 \pm 0.012 \pm 0.09$, $|A_{\parallel}|^2 = 0.233 \pm 0.013 \pm 0.008$, $|A_{\perp}|^2 = 0.181 \pm 0.012 \pm 0.008$, $\arg(A_{\parallel}) = 2.888 \pm 0.090 \pm 0.008$ radians, and $\arg(A_{\perp}) = 0.239 \pm 0.064 \pm 0.010$ radians. The difference between $\arg(A_{\parallel})$ and $\arg(A_{\perp})$ is 2.649 ± 0.110 radians, which is shifted from π by more than 4σ ; this can be interpreted as evidence for the existence of the final state interaction. The amplitude values are used in triple product correlations to obtain asymmetries of $A_T^{(1)} = 0.101 \pm 0.033 \pm 0.007$ and $A_T^{(2)} = -0.102 \pm 0.032 \pm 0.003$ for B^0 meson decays, and $\bar{A}_T^{(1)} = 0.056 \pm 0.030 \pm 0.006$ and $\bar{A}_T^{(2)} = -0.091 \pm 0.028 \pm 0.003$ for \bar{B}^0 meson decays. The time dependent angular analysis gives the measurements of CP violating parameters $\sin 2\phi_1$ and $\cos 2\phi_1$ to be $0.30 \pm 0.32 \pm 0.02$ and $-0.31 \pm 0.91 \pm 0.10$, respectively. The value of $\cos 2\phi_1$ is $-0.56 \pm 0.86 \pm 0.11$ if $\sin 2\phi_1$ is fixed at the world average value (0.731).

PACS numbers: 13.25.Hq, 14.40.Nd

INTRODUCTION

An angular analysis of B meson decay to two vector mesons can be a sensitive probe of new physics. Since the analysis is equivalent to the simultaneous study of three decay modes corresponding to the possible helicity states of two vector mesons, the effect of the new physics that might appear in the interference among the states can be observed cleanly with the cancellation of most systematic effects.

Recently, the anomaly in the decay amplitudes in $B \rightarrow \phi K^*$ has been reported where the longitudinal amplitude is lower than the Standard Model prediction[1]. For the precise study of such anomalies, a comparison with theoretically clean reference modes is necessary. The decay $B^0 \rightarrow J/\psi K^{*0}$ is an ideal mode for this purpose since it is a tree dominated mode with a very low penguin contribution where the theoretical ambiguity on the CP-sensitive parameter $\sin 2\phi_1$ [2] is less than 1% level[3].

There are three classes of parameters that can be used to probe new physics obtained through the angular analysis. The first is the measurement of the decay amplitudes of the three helicity states. They can be obtained by the time-integrated angular analysis to flavor specific decays. The comparison of the amplitudes between flavor-separated samples probes the direct CP violation. The second is the triple product correlation, which can be extracted from the measured decay amplitudes. This quantity is sensitive to the T-violation. The third class is comprised of the CP parameters ($\sin 2\phi_1$ and $\cos 2\phi_1$) that are measured through the time-dependent angular analysis. In particular, the measurement of $\cos 2\phi_1$, which appears in the time-dependent interference terms, is important both to solve the two-fold ambiguity in $2\phi_1$ and to test the consistency of this determination with the more precise value from other $b \rightarrow c\bar{c}s$ decays.

In this paper, we report the measurements of all three classes of parameters for $B^0 \rightarrow J/\psi K^{*0}$ decays.

DATA SAMPLE

The data sample used in this analysis corresponds to an integrated luminosity of 253 fb^{-1} recorded with the Belle detector[4] at the KEKB electron-positron collider[5]. Events are required to satisfy the hadronic event selection criteria[2] and have $R_2 < 0.5$, where R_2 is the ratio of the second to zeroth Fox-Wolfman event shape moments[6].

The reconstruction of J/ψ candidates is performed using the dilepton decays $J/\psi \rightarrow e^+e^-$ and $\mu^+\mu^-$. For the e^+e^- mode, a track is identified as an electron or positron by a comparison of the energy measured in the electromagnetic calorimeter (ECL) with the momentum measured in the central drift chamber (CDC), the shape of the cluster energy deposit in the ECL, the specific ionization (dE/dx) measured in the CDC, and the light yield in the aerogel Čerenkov counters (ACC). The likelihoods that the track is an electron or a hadron are determined from these measurements. The likelihood ratio is required to be consistent with the electron hypothesis. To correct for energy lost by final state radiation, the energy of any cluster in the ECL within 0.05 radians of the initial track momentum is added to that of the track. The invariant mass of each so-augmented electron-positron pair is calculated, and the pair is associated with $J/\psi \rightarrow e^+e^-$ if the mass is in the range $2.95 \text{ GeV}/c^2 < M(e^+e^-) < 3.15 \text{ GeV}/c^2$. Tracks are identified as muons rather than hadrons by means of likelihoods based on (i) a comparison of the number of layers with associated hits in the muon detector (KLM) with the number expected based

on momentum and (ii) the energy of the associated hit in the ECL. An oppositely charged pair of muons is identified as arising from $J/\psi \rightarrow \mu^+\mu^-$ if the invariant mass is in the range $3.05 \text{ GeV}/c^2 < M(\mu^+\mu^-) < 3.15 \text{ GeV}/c^2$. To improve the momentum resolution, a kinematic fit that uses the J/ψ mass as a constraint is performed on J/ψ candidates passing the above selections.

Candidate K^{*0} mesons are reconstructed using the decay modes $K^{*0} \rightarrow K^+\pi^-$ and $K^{*0} \rightarrow K_S^0\pi^0$. A track is identified as a kaon based on the ratio of its likelihoods to be a kaon *vs* a pion. These likelihoods are obtained from the measurements mentioned above from the TOF, CDC and ACC detectors. Tracks that are not identified as kaons and not used as leptons in the J/ψ reconstruction are treated as charged pion candidates. K_S^0 candidates are reconstructed from pairs of oppositely charged tracks that satisfy three conditions: 1) the distance of closest approach of each track to the nominal interaction point is larger than 0.03 cm, 2) the angle between the K_S^0 momentum vector and the vector displacement of the K_S^0 vertex point from the J/ψ vertex is less than 0.15 radians, and 3) the reconstructed decay vertex of the K_S^0 is at least 0.1 cm away from the interaction point. Each pair with an invariant mass satisfying $0.47 \text{ GeV}/c^2 < M(\pi^+\pi^-) < 0.52 \text{ GeV}/c^2$ is identified as a K_S^0 meson. To improve the mass resolution, the pion momenta are re-fitted, constraining both tracks to originate at the reconstructed K_S^0 vertex.

Candidate π^0 mesons are reconstructed from clusters in the ECL that are unmatched to charged tracks and having energy greater than 40 MeV. A photon pair with an invariant mass in the range $0.125 \text{ GeV}/c^2 < M(\gamma\gamma) < 0.145 \text{ GeV}/c^2$ is identified as a π^0 . A mass-constrained fit is performed to obtain the momentum of the π^0 meson. A $K\pi$ pair is considered a K^* candidate if the invariant mass of the pair is within $74 \text{ MeV}/c^2$ of the nominal $K^*(892)$ mass.

Candidate B^0 mesons are reconstructed by selecting events with a J/ψ and a K^* meson and examining two quantities in the center-of-mass of the $\Upsilon(4S)$: the beam-constrained mass (M_{bc}) and the energy difference between the B candidate and the beam energy (ΔE). The beam-constrained mass, which is the invariant mass of a reconstructed J/ψ and K^* calculated taking the energy to be the beam energy, is required to be in the range $5.27 - 5.29 \text{ GeV}/c^2$. For the mode with $K^{*0} \rightarrow K^+\pi^-$, $|\Delta E|$ is required to be less than 30 MeV, while ΔE is required to satisfy $-50 \text{ MeV} < \Delta E < 30 \text{ MeV}$ for $K^{*0} \rightarrow K_S^0\pi^0$.

To eliminate slow π^0 backgrounds, the angle θ_{K^*} of the kaon with respect to the K^* direction in the K^* rest frame is required to satisfy $\cos\theta_{K^*} < 0.8$. This is equivalent to demanding that the π^0 momentum be greater than $175 \text{ MeV}/c$. When an event contains more than one candidate passing the above requirements, the combination for which both M_{bc} and ΔE are the closest to the B^0 mass and zero, respectively, is selected. After all the selections, **8194** $K^{*0} \rightarrow K^+\pi^-$ candidates and **354** $K^{*0} \rightarrow K_S^0\pi^0$ candidates remain. Figure 1 shows the distributions of M_{bc} and ΔE for the samples.

MEASUREMENT OF DECAY AMPLITUDES

The decay amplitudes of $B \rightarrow J/\psi K^*$ decays are measured in the transversity basis[7]. The definition of the angles is shown in Fig. 2. The direction of motion of the J/ψ in the rest frame of the B candidate is defined to be the x -axis. The y -axis is chosen along the direction of the projection of the K momentum into the plane perpendicular to the x -axis in the B rest frame. The x - y plane contains the momenta of the J/ψ , the K , and the π mesons. The z -axis is then perpendicular to the x - y plane according to the right-hand rule.

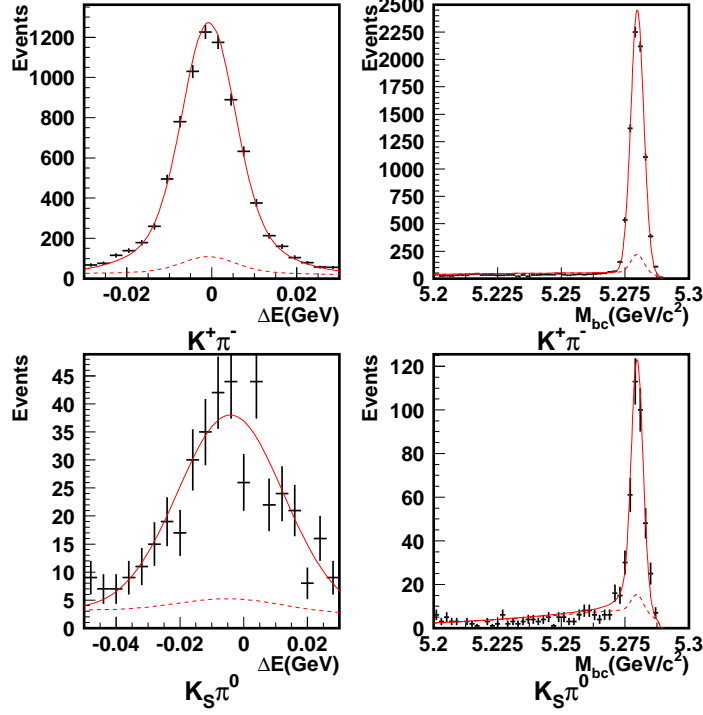


FIG. 1: ΔE and M_{bc} distributions for reconstructed $B^0 \rightarrow J/\psi K^{*0}(K^+\pi^-)$ (upper figures) and $B^0 \rightarrow J/\psi K^{*0}(K_S^0\pi^0)$ (lower figures) samples. Solid lines show the results of two dimensional fits while dashed lines are estimated background contaminations.

The angle between the the positive lepton (l^+) daughter and the z -axis in the J/ψ rest frame is defined as θ_{tr} . The angle between the x -axis and the projection of the l^+ momentum onto the x - y plane is defined as ϕ_{tr} in the same frame. The angle θ_{K^*} is defined as described in the previous section.

The distribution of these three angles for $B \rightarrow J/\psi K^*$ decays is described in terms of three amplitudes[8]:

$$\begin{aligned} \frac{1}{\Gamma} \frac{d\Gamma}{d\cos\theta_{tr}d\cos\theta_{K^*}d\phi_{tr}} &= \frac{9}{32\pi} \times [2\cos^2\theta_{K^*}(1 - \sin^2\theta_{tr}\cos^2\phi_{tr})|A_0|^2 \\ &+ \sin^2\theta_{K^*}(1 - \sin^2\theta_{tr}\sin^2\phi_{tr})|A_{\parallel}|^2 \\ &+ \sin^2\theta_{K^*}\sin^2\theta_{tr}|A_{\perp}|^2 \\ &+ \eta\sin^2\theta_{K^*}\sin 2\theta_{tr}\sin\phi_{tr}Im(A_{\parallel}^*A_{\perp}) \\ &- \frac{1}{\sqrt{2}}\sin 2\theta_{K^*}\sin^2\theta_{tr}\sin 2\phi_{tr}Re(A_0^*A_{\parallel}) \\ &+ \eta\frac{1}{\sqrt{2}}\sin 2\theta_{K^*}\sin 2\theta_{tr}\cos\phi_{tr}Im(A_0^*A_{\perp})], \end{aligned} \quad (1)$$

where A_0 , A_{\parallel} and A_{\perp} are the complex amplitudes of the three helicity states in the trasversity basis, and $\eta = +1$ (-1) for B^0 ($\overline{B^0}$). The coefficient $|A_0|^2$ denotes the longitudinal

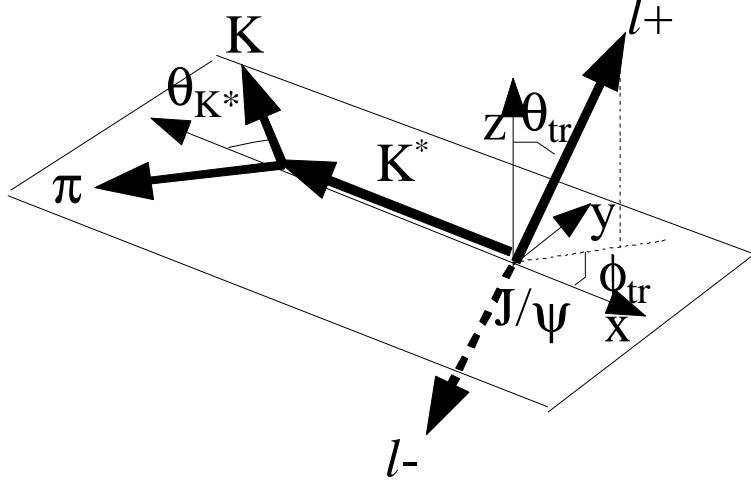


FIG. 2: The definition of transversity angles.

polarization of J/ψ while $|A_{\perp}|^2$ ($|A_{\parallel}|^2$) gives the transverse polarization component along the z -axis (y -axis). In the decay mode where $K^{*0} \rightarrow K_S^0 \pi^0$, $|A_0|^2 + |A_{\parallel}|^2$ ($|A_{\perp}|^2$) is the component corresponding to the CP-even (CP-odd) state.

The amplitudes are determined by fitting this function to the measured three-dimensional distribution in θ_{tr} , ϕ_{tr} and θ_{K^*} , taking into account the detection efficiency and background. The resolution of the angular measurements is estimated by Monte Carlo (MC) simulation and found to be typically less than 0.02 radians. The value of η is determined from the charge of pions or kaons used in the K^* reconstruction. We use only $B^0 \rightarrow J/\psi K^{*0} (K^+ \pi^-)$ decays for the measurement since η is not well-defined in $B^0 \rightarrow J/\psi K^{*0} (K_S^0 \pi^0)$ decays.

The fit is performed using an unbinned maximum likelihood method. The probability density function (\mathcal{G}) is defined using the theoretical distribution in (1) and can be expressed as

$$\begin{aligned} \mathcal{G}(x, y, z, M_{bc}, \Delta E) = & N \times [f_{sig}(M_{bc}, \Delta E) \times \epsilon(x, y, z) \times \frac{1}{\Gamma} \frac{d^3\Gamma}{dx dy dz}(x, y, z) \\ & + \sum_i f_{cf}^i(M_{bc}, \Delta E) \times \mathcal{A}_{cf}(x, y, z) \\ & + f_{nr}(M_{bc}, \Delta E) \times \mathcal{A}_{nr}(x, y, z) \\ & + f_{cb}(M_{bc}, \Delta E) \times \mathcal{A}_{cb}(x, y, z)], \end{aligned} \quad (2)$$

where $x = \cos\theta_{tr}$, $y = \phi_{tr}$, and $z = \cos\theta_{K^*}$, N is the normalization factor of \mathcal{G} , $\epsilon(x, y, z)$ is the detection efficiency as a function of the three angles, and \mathcal{A}_{cf} , \mathcal{A}_{nr} , \mathcal{A}_{cb} are the angular shapes for the cross-feed, non-resonant and combinatorial backgrounds, respectively.

Here, $f_{sig}(M_{bc}, \Delta E)$, $f_{cf}^i(M_{bc}, \Delta E)$, $f_{nr}(M_{bc}, \Delta E)$, and $f_{cb}(M_{bc}, \Delta E)$ are the fractions of signal events, cross-feed contamination, non-resonant contamination and combinatorial background, respectively, as a function of M_{bc} and ΔE . These fractions are obtained with a data subsample of 140 fb^{-1} by the procedure given in Ref.[9] with an improvement to use both M_{bc} and ΔE in the fits.

The detection efficiency function $\epsilon(x, y, z)$ is obtained from a large MC sample of 6 million events generated polarized with the decay amplitudes set at the values of the previous

TABLE I: Summary of measured decay amplitudes.

	Flavor averaged	B^0	\overline{B}^0
$ A_0 ^2$	0.585 ± 0.012	0.581 ± 0.016	0.589 ± 0.016
$ A_{\parallel} ^2$	0.233 ± 0.013	0.220 ± 0.018	0.246 ± 0.018
$ A_{\perp} ^2$	0.181 ± 0.012	0.199 ± 0.018	0.164 ± 0.017
$\arg(A_{\parallel})$	2.888 ± 0.090	2.937 ± 0.136	2.854 ± 0.120
$\arg(A_{\perp})$	0.239 ± 0.064	0.303 ± 0.090	0.182 ± 0.089

measurement[9]. Events are histogrammed in a $20 \times 20 \times 20$ grid in the $\cos\theta_{tr} - \phi_{tr} - \cos\theta_{K^*}$ cube. The distribution is fitted to the product of three one-dimensional polynomials.

The angular distribution function for the cross-feed background (\mathcal{A}_{cf}) is determined from MC simulation. The function for the non-resonant production (\mathcal{A}_{nr}) is determined from events in the sideband of the $K\pi$ mass distribution ($1.0 \text{ GeV}/c^2 < M(K\pi) < 1.3 \text{ GeV}/c^2$). The distribution for the combinatorial background (\mathcal{A}_{cb}) is obtained from events in the sideband with $5.2 \text{ GeV}/c^2 < M_{bc} < 5.26 \text{ GeV}/c^2$. These normalized distributions are parameterized as the product of three one-dimensional polynomials whose parameters are determined from the fit.

In the fit, the phase of A_0 is defined to be zero relative to those of the other amplitudes since the overall phase of the decay amplitudes is arbitrary. The other five parameters, $|A_0|^2$, $|A_{\parallel}|^2$, $|A_{\perp}|^2$, $\arg(A_{\parallel})$ and $\arg(A_{\perp})$ are free parameters in the fit. The normalization condition of the amplitudes

$$|A_0|^2 + |A_{\parallel}|^2 + |A_{\perp}|^2 = 1 \quad (3)$$

is taken into account by adopting the extended likelihood defined as

$$-\ln L = -\sum_{i=1}^{N_{obs}} \ln \mathcal{G}_i + N_{exp} - N_{obs} \ln(N_{exp}) \quad (4)$$

where N_{obs} is the number of events used for the fit. N_{exp} is defined to be $N_{obs} \cdot (|A_0|^2 + |A_{\parallel}|^2 + |A_{\perp}|^2)$ to incorporate the normalization condition. The normalization N of \mathcal{G} is recalculated by numerical integration whenever the fit parameters change. The parameter values determined from the fit are summarized in Table I and the projected angular distributions are shown in Fig. 3. The distributions are corrected for the effects of detector acceptance and backgrounds. Small discrepancies from 0 or π are observed in $\arg(A_{\parallel})$ and $\arg(A_{\perp})$. The difference of these two phases is 2.649 ± 0.110 radians which is shifted from π by more than 4σ . This is read to be evidence for the existence of final state interaction.

There are two choices for the imaginary phases of the helicity amplitudes[10]. We obtain the above values by taking the conventional choice of the phases noted as solution I in Ref.[10]. If the alternative set of the phases is used, the imaginary phases become $\arg(A_{\parallel}) \rightarrow -\arg(A_{\parallel})$, and $\arg(A_{\perp}) \rightarrow \pi - \arg(A_{\perp})$.

The parameter values are also measured for B^0 (4121 candidates) and \overline{B}^0 (4073 candidates) samples separately and the results are given in Table I. The measured values are consistent between both B^0 and \overline{B}^0 decays, indicating no evidence for direct CP violation.

Systematic uncertainties in the fit are determined as follows: 1) efficiency function (MC statistics and effect of polarization), 2) angular distribution functions for backgrounds, 3)

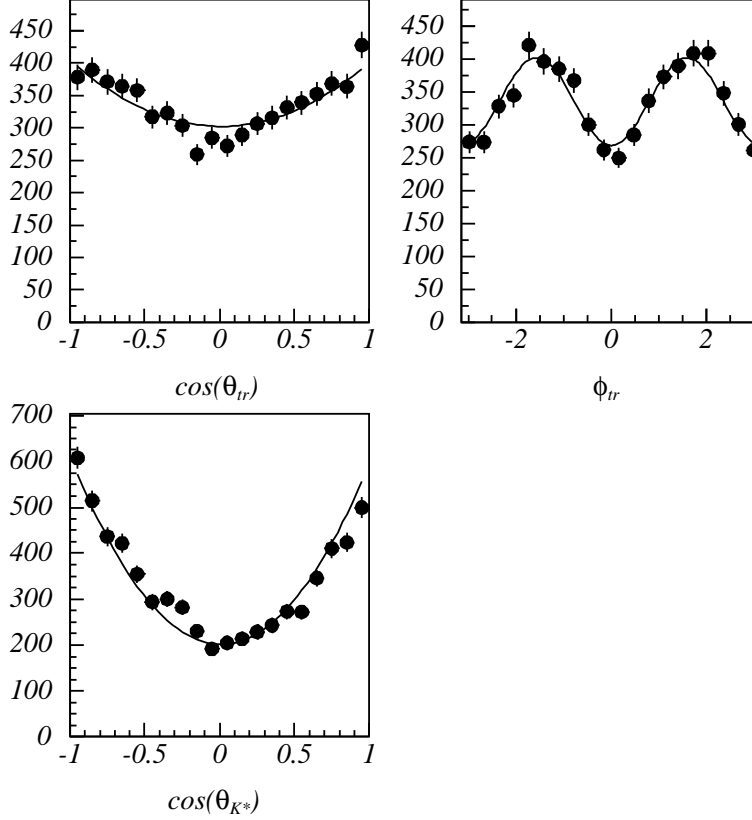


FIG. 3: Distributions of projected angles. Solid lines show results of the fit. The data points are corrected for the detector efficiency and the backgrounds are subtracted.

TABLE II: Systematic errors in the measurement of decay amplitudes.

Item	$ A_0 ^2$	$ A_{ } ^2$	$ A_{\perp} ^2$	$\arg(A_{ })$	$\arg(A_{\perp})$
Efficiency	0.003	0.002	0.001	0.001	0.003
PDF for backgrounds	0.002	0.002	0.002	0.004	0.006
Background fractions	0.001	0.002	0.003	0.001	0.002
Slow pion efficiency	0.008	0.007	0.007	0.006	0.007
Polarization in NR	0.002	0.002	0.003	0.003	0.003
Total	0.009	0.008	0.008	0.008	0.010

background fractions, 4) slow pion efficiency, and 5) polarization effect in non-resonant decays. These contributions to the systematic error are summarized in Table II. The dominant contribution arises from the uncertainty in the detection efficiency for slow pions. This is estimated by comparing the results with a cut at $\cos\theta_{K^*} < 0.9$. The angular shape in non-resonant backgrounds is a potential source of uncertainty since it might contain tails of other resonances whose polarization is different. The uncertainty is determined by comparing with the results obtained assuming the angular distribution to be that of phase space decay.

TRIPLE PRODUCT CORRELATIONS

The T-violating triple product correlations are sensitive probes to new physics effects[11]. The asymmetry of the triple product is defined as

$$A_T = \frac{\Gamma(\vec{v}_1 \cdot (\vec{v}_2 \times \vec{v}_3) > 0) - \Gamma(\vec{v}_1 \cdot (\vec{v}_2 \times \vec{v}_3) < 0)}{\Gamma(\vec{v}_1 \cdot (\vec{v}_2 \times \vec{v}_3) > 0) + \Gamma(\vec{v}_1 \cdot (\vec{v}_2 \times \vec{v}_3) < 0)} \quad (5)$$

where \vec{v}_1 is the momentum of J/ψ or K^{*0} meson, while \vec{v}_2 and \vec{v}_3 are the polarization vectors of J/ψ and K^{*0} meson, respectively. Experimentally, two asymmetries can be defined using the measured decay amplitudes for B^0 decays, as follows:

$$A_T^{(1)} = \frac{Im(A_\perp A_0^*)}{A_0^2 + A_\parallel^2 + A_\perp^2} \quad A_T^{(2)} = \frac{Im(A_\perp A_\parallel^*)}{A_0^2 + A_\parallel^2 + A_\perp^2}. \quad (6)$$

The corresponding asymmetries for \overline{B}^0 decays are defined as $\bar{A}_T^{(1)}$ and $\bar{A}_T^{(2)}$. The Standard Model predicts tiny values for these asymmetries and no difference between B^0 and \overline{B}^0 mesons.

By putting the measured amplitude values in Eq. 6, the triple product asymmetries are obtained as

$$\begin{aligned} A_T^{(1)} &= 0.101 \pm 0.033 \pm 0.007 \\ A_T^{(2)} &= -0.102 \pm 0.032 \pm 0.003 \\ \bar{A}_T^{(1)} &= 0.056 \pm 0.030 \pm 0.006 \\ \bar{A}_T^{(2)} &= -0.091 \pm 0.028 \pm 0.003 \end{aligned}$$

As seen, all the obtained triple product asymmetries are close to zero, furthermore, no difference between A_T 's and \bar{A}_T 's is observed.

MEASUREMENT OF CP VIOLATION PARAMETERS

The CP violation parameters $\sin 2\phi_1$ and $\cos 2\phi_1$ are measured by studying the angular distributions in the CP decay mode $B^0 \rightarrow J/\psi K^{*0}; K^{*0} \rightarrow K_S^0 \pi^0$ as a function of the decay time difference between B^0 and \overline{B}^0 (Δt). The Δt -dependent form of Eq. 1 becomes[8]:

$$\frac{d^4\Gamma(\theta_{tr}, \phi_{tr}, \theta_{K^*}, \Delta t)}{d\cos\theta_{tr}d\phi_{tr}d\cos\theta_{K^*}d\Delta t} = \frac{e^{-|\Delta t|/\tau_{B^0}}}{2\tau_{B^0}} \sum_{i=1}^6 g_i(\theta_{tr}, \phi_{tr}, \theta_{K^*}) a_i(\Delta t) \quad (7)$$

where τ_B is the lifetime of a B^0 meson, and the angular terms are expressed as:

$$g_1 = 2\cos^2\theta_{K^*}(1 - \sin^2\theta_{tr}\cos^2\phi_{tr}) \quad (8)$$

$$g_2 = \sin^2\theta_{K^*}(1 - \sin^2\theta_{tr}\sin^2\phi_{tr}) \quad (9)$$

$$g_3 = \sin^2\theta_{K^*}\sin^2\theta_{tr} \quad (10)$$

$$g_4 = \frac{-1}{\sqrt{2}}\sin 2\theta_{K^*}\sin^2\theta_{tr}\sin 2\phi_{tr} \quad (11)$$

$$g_5 = \sin^2\theta_{K^*}\sin 2\theta_{tr}\sin\phi_{tr} \quad (12)$$

$$g_6 = \frac{1}{\sqrt{2}}\sin 2\theta_{K^*}\sin 2\theta_{tr}\cos\phi_{tr} \quad (13)$$

while the amplitude terms are expressed as:

$$a_1 = |A_0|^2(1 + \eta \sin 2\phi_1 \sin \Delta m \Delta t) \quad (14)$$

$$a_2 = |A_{\parallel}|^2(1 + \eta \sin 2\phi_1 \sin \Delta m \Delta t) \quad (15)$$

$$a_3 = |A_{\perp}|^2(1 - \eta \sin 2\phi_1 \sin \Delta m \Delta t) \quad (16)$$

$$a_4 = \text{Re}(A_{\parallel}^* A_0)(1 + \eta \sin 2\phi_1 \sin \Delta m \Delta t) \quad (17)$$

$$a_5 = \eta \text{Im}(A_{\parallel}^* A_{\perp}) \cos \Delta m \Delta t - \eta \text{Re}(A_{\parallel}^* A_{\perp}) \cos 2\phi_1 \sin \Delta m \Delta t \quad (18)$$

$$a_6 = \eta \text{Im}(A_0^* A_{\perp}) \cos \Delta m \Delta t - \eta \text{Re}(A_0^* A_{\perp}) \cos 2\phi_1 \sin \Delta m \Delta t. \quad (19)$$

Here, Δm is a $B^0 - \overline{B}^0$ mixing parameter. η is +1 for B^0 and -1 for \overline{B}^0 . A_0 , A_{\parallel} and A_{\perp} are the decay amplitudes given in the previous section. Two CP violation parameters appear in the formula, *viz*, $\sin 2\phi_1$ and $\cos 2\phi_1$. The latter parameter appears in the interference terms a_5 and a_6 .

The procedures to measure the decay time difference and to determine the flavor of decaying B^0 meson are described elsewhere[2]. The values of $\sin 2\phi_1$ and $\cos 2\phi_1$ are determined by fitting the function to the measured angles and Δt , taking into account the detection efficiency and background. The fit is done using an unbinned maximum likelihood method. The probability density function for an event is defined as

$$\begin{aligned} \mathcal{P} = & f_{sig}(M_{bc}, \Delta E) \epsilon(\theta_{tr}, \phi_{tr}, \theta_{K^*}) \frac{d^4 \Gamma(\theta_{tr}, \phi_{tr}, \theta_{K^*}, \Delta t)}{d \cos \theta_{tr} d \phi_{tr} d \cos \theta_{K^*} d \Delta t} \\ & + \frac{e^{-|\Delta t|/\tau_{B^0}}}{2\tau_{B^0}} \left\{ \sum_i f_{cf}^i(M_{bc}, \Delta E) \mathcal{A}_{cf}(\theta_{tr}, \phi_{tr}, \theta_{K^*}) \right. \\ & \quad \left. + f_{nr}(M_{bc}, \Delta E) \mathcal{A}_{nr}(\theta_{tr}, \phi_{tr}, \theta_{K^*}) \right\} \\ & + \delta(\Delta t) f_{cb}(M_{bc}, \Delta E) \mathcal{A}_{cb}(\theta_{tr}, \phi_{tr}, \theta_{K^*}). \end{aligned} \quad (20)$$

Here, f_{sig} , f_{cf} , f_{nr} and f_{cb} are the fractions of signal, cross feed, non-resonant production, and combinatorial background components, respectively, while \mathcal{A}_{cf} , \mathcal{A}_{nr} and \mathcal{A}_{cb} are the corresponding three-dimensional angular shape functions. Also, ϵ is a three dimensional detection efficiency function for the signal. These functions are the same as those used in the decay amplitude measurement. The flavor tagging procedure gives the flavor q of tag-side B meson and the probability w that this flavor determination is incorrect. To account for the effect of wrong tagging in this fit, η is replaced with $-q(1 - 2w)$ within the signal angular distribution in Eq. 20.

Each term in \mathcal{P} is then convolved with the appropriate resolution functions separately for the signal, backgrounds having the B^0 lifetime (namely, cross feeds and non-resonant production) and the combinatorial background with a zero-lifetime δ -function shape, which takes into account the effect of vertex position smearing caused by the detector resolution, charmed meson decays, and poorly reconstructed tracks. The resolution parameters are calculated event by event using the energy of the reconstructed B meson, the direction of the B meson with respect to the beam axis and the momentum of the B meson in the center-of-mass frame [12].

In the fit, the helicity amplitudes are fixed at the values determined in the previous section. The values of the lifetime and mixing parameter are set at the values given in Ref. [13]. The CP parameters $\sin 2\phi_1$ and $\cos 2\phi_1$ are the only free parameters in the fit. From the fit to the data, we obtain

$$\sin 2\phi_1 = 0.30 \pm 0.32 \pm 0.02,$$

TABLE III: Systematic errors in the measured CP parameters.

Item	$\sin 2\phi_1$	$\cos 2\phi_1$	$\cos 2\phi_1$ ($\sin 2\phi_1 = 0.731$)
Vertexing	0.008	0.050	0.051
Resolution parameters	0.005	0.010	0.010
Wrong tagging fractions	0.009	0.061	0.062
δ -function for BG	0.006	0.004	0.005
τ_B and Δm	0.004	0.010	0.010
Decay amplitudes	0.005	0.041	0.048
Angular shape for backgrounds	0.007	0.025	0.044
Background fraction	0.011	0.021	0.021
Total	0.020	0.096	0.107

$$\cos 2\phi_1 = -0.31 \pm 0.90 \pm 0.10.$$

When we fix the value of $\sin 2\phi_1$ at the world average value (0.731)[14], the value of $\cos 2\phi_1$ becomes

$$\cos 2\phi_1 = -0.56 \pm 0.86 \pm 0.11 \quad (21)$$

We obtain the above values by taking a set of the phases given in the previous section. If the alternative set of the phases is used in the fit, the sign of $\cos 2\phi_1$ flips, giving $\cos 2\phi_1 = +0.31 \pm 0.86 \pm 0.11$, while $\sin 2\phi_1$ does not change.

Systematic uncertainties in the fit are determined in the same manner as those in $b \rightarrow c\bar{c}s$ $\sin 2\phi_1$ measurement[2]. In addition, the uncertainties that come from the angular analysis (decay amplitudes, background angular shapes, and background fractions) are estimated. The uncertainty in decay amplitudes are determined by varying the values by one standard deviation. The uncertainty in the background fractions and angular shapes are estimated in the same manner as that in the decay amplitude measurement.

The raw asymmetry in the measured Δt between samples tagged as B^0 and \overline{B}^0 is shown in Fig. 4 together with the result of the fit.

The systematics in the fit are checked by applying the same fitting procedure to the sample of $B \rightarrow J/\psi K^{*0}(K^+\pi^-)$ decays. We obtain following values for parameters $\sin 2\phi_1$ and $\cos 2\phi_1$:

$$\begin{aligned} \text{“}\sin 2\phi_1\text{”} &= -0.037 \pm 0.068 \\ \text{“}\cos 2\phi_1\text{”} &= 0.103 \pm 0.179 \end{aligned}$$

These are consistent with zero, as expected.

CONCLUSION

A full angular analysis is performed for $B^0 \rightarrow J/\psi K^{*0}$ ($K^{*0} \rightarrow K^+\pi^-$) decays. The complex decay amplitudes of three helicity final states are measured by the simultaneous fit to three transversity angles and the best fit values are $|A_0|^2 = 0.585 \pm 0.012 \pm 0.009$, $|A_{\parallel}|^2 = 0.233 \pm 0.013 \pm 0.008$, $|A_{\perp}|^2 = 0.181 \pm 0.012 \pm 0.008$, $\arg(A_{\parallel}) = 2.888 \pm 0.090 \pm 0.008$

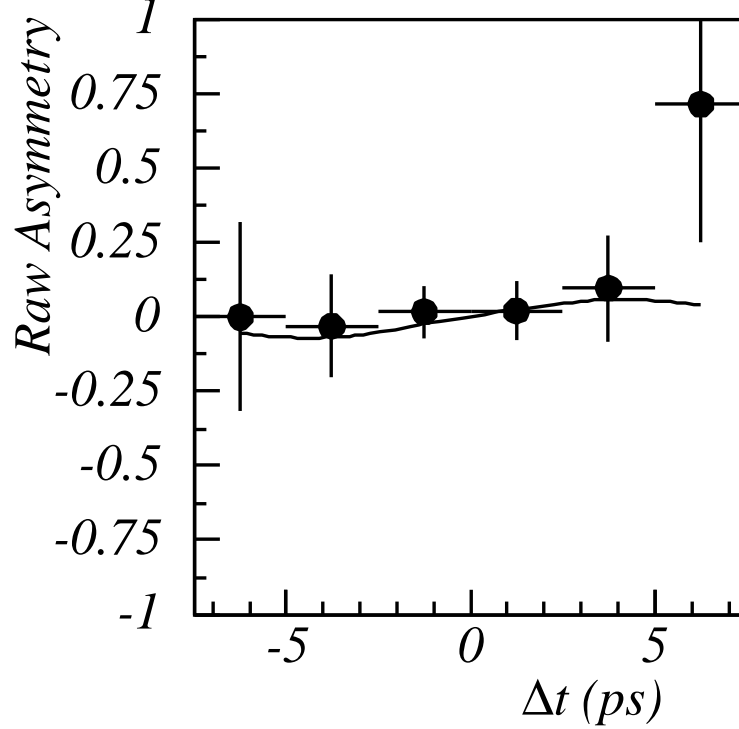


FIG. 4: Raw asymmetry in measured Δt between samples tagged as B^0 and \overline{B}^0 . The solid line shows the projection of the fit.

radians, and $\arg(A_{\perp}) = 0.239 \pm 0.064 \pm 0.010$ radians, where $\arg(A_0)$ is defined to be zero. There are two choices for the set of imaginary phases. We obtain the above values by taking the conventional choice of phases. The measured value of $|A_{\perp}|^2$ shows that the CP even component dominates in $B^0 \rightarrow J/\psi K^{*0}; K^{*0} \rightarrow K_S^0 \pi^0$ decays. Small discrepancies from π or 0 are observed in $\arg(A_{\parallel})$ and $\arg(A_{\perp})$, respectively. The difference of these two phases is calculated to be 2.649 ± 0.110 radians and the shift from π is more than 4σ . This is read to be an evidence for the existence of final state interactions. The amplitudes are also measured for B^0 and \overline{B}^0 decays separately. The best fit values are consistent between them and no direct CP violating effect is observed.

The measured amplitudes are converted into the asymmetries in the triple product correlations: the best fit values are $A_T^{(1)} = 0.101 \pm 0.033 \pm 0.007$ and $A_T^{(2)} = -0.102 \pm 0.032 \pm 0.003$ for B^0 mesons, and $\bar{A}_T^{(1)} = 0.056 \pm 0.030 \pm 0.006$ and $\bar{A}_T^{(2)} = -0.091 \pm 0.028 \pm 0.003$ for \overline{B}^0 mesons. The differences between two asymmetries for B^0 and \overline{B}^0 mesons are consistent with zero and no new physics effects are observed.

The time dependent angular analysis is performed for $B^0 \rightarrow J/\psi K^{*0}$ ($K^{*0} \rightarrow K_S^0 \pi^0$) decays. By the simultaneous fit to the three transversity angles and Δt , the CP violation parameters $\sin 2\phi_1$ and $\cos 2\phi_1$ are determined to be $\sin 2\phi_1 = 0.30 \pm 0.32 \pm 0.02$ and $\cos 2\phi_1 = -0.31 \pm 0.91 \pm 0.10$. Fixing $\sin 2\phi_1$ at the world average value (0.73) gives $\cos 2\phi_1 = -0.56 \pm 0.86 \pm 0.11$. The decay amplitudes are fixed at the values measured in the time integrated fit with the conventional choice of imaginary phases. When taking the other choice, the sign of $\cos 2\phi_1$ flips; however, we cannot put a constraint on the sign of $\cos 2\phi_1$ regardless of the choice of the imaginary phase set.

TABLE IV: Comparison of obtained decay amplitudes and CP violation parameters with previous measurements. Here, the sign of $\cos 2\phi_1$ of Belle measurements is put to be consistent with BaBar's choice of phases.

	This Measurement	Belle[9][16]	BaBar[15]
Luminosity	253fb^{-1}	29fb^{-1} (78 for CP)	83fb^{-1} (113 for CP)
$ A_0 ^2$	$0.585 \pm 0.012 \pm 0.009$	$0.62 \pm 0.02 \pm 0.03$	$0.566 \pm 0.012 \pm 0.005$
$ A_{\parallel} ^2$	$0.233 \pm 0.013 \pm 0.008$	-	$0.204 \pm 0.015 \pm 0.005$
$ A_{\perp} ^2$	$0.181 \pm 0.012 \pm 0.008$	$0.19 \pm 0.02 \pm 0.03$	$0.230 \pm 0.015 \pm 0.004$
$\arg(A_{\parallel})$	$2.888 \pm 0.090 \pm 0.008$	$2.83 \pm 0.19 \pm 0.08$	$2.729 \pm 0.101 \pm 0.052$
$\arg(A_{\perp})$	$0.239 \pm 0.064 \pm 0.010$	$-0.09 \pm 0.13 \pm 0.06$	$0.184 \pm 0.070 \pm 0.046$
$\sin 2\phi_1$	$0.30 \pm 0.32 \pm 0.02$	$0.13 \pm 0.51 \pm 0.06$	-0.10 ± 0.57
$\cos 2\phi_1$	$+0.31 \pm 0.91 \pm 0.11$	$+1.40 \pm 1.28 \pm 0.19$	$+3.32^{+0.76}_{-0.96} \pm 0.27$

Table IV shows the comparison with previous measurements. The measured decay amplitudes are consistent among all measurements.

We thank the KEKB group for the excellent operation of the accelerator, the KEK Cryogenics group for the efficient operation of the solenoid, and the KEK computer group and the National Institute of Informatics for valuable computing and Super-SINET network support. We acknowledge support from the Ministry of Education, Culture, Sports, Science, and Technology of Japan and the Japan Society for the Promotion of Science; the Australian Research Council and the Australian Department of Education, Science and Training; the National Science Foundation of China under contract No. 10175071; the Department of Science and Technology of India; the BK21 program of the Ministry of Education of Korea and the CHEP SRC program of the Korea Science and Engineering Foundation; the Polish State Committee for Scientific Research under contract No. 2P03B 01324; the Ministry of Science and Technology of the Russian Federation; the Ministry of Education, Science and Sport of the Republic of Slovenia; the National Science Council and the Ministry of Education of Taiwan; and the U.S. Department of Energy.

* on leave from Nova Gorica Polytechnic, Nova Gorica

- [1] K.Abe, *et al.* (Belle Collaboration), “Measurement of Polarization in $B \rightarrow \phi K^*$ Decays”, BELLE-CONF-0419 (2004), submitted to this conference; K.F.Chen, *et al.* (Belle Collaboration), Phys. Rev. Lett. **91**, 201801 (2003); J.G.Smith, *et al.* (BaBar Collaboration), hep-ex/040663 (2004).
- [2] K.Abe *et al.* (Belle Collaboration), “Improved measurements of time-dependent decay-rate asymmetries in $B^0 \rightarrow J/\psi K_S^0$ and other $b \rightarrow c\bar{c}s$ transitions,” BELLE-CONF-0436, (2004) submitted to this conference; K.Abe *et al.* (Belle Collaboration), Phys. Rev. D **66**, 071102(R) (2002); K.Abe *et al.* (Belle Collaboration), Phys. Rev. Lett. **87**, 091802 (2001).
- [3] X.Y.Pharm and Z.Z.Xing, Phys.Lett. **B458**, 375 (1999).
- [4] A.Abashian *et al.* (Belle Collaboration), Nucl. Inst. and Meth. **A479**, 117 (2002).
- [5] S. Kurokawa and E. Kikutani, Nucl. Instr. and Meth. **A499**, 1 (2003).

- [6] G.Fox and S.Wolfram, Phys. Rev. Lett **41**, 1581 (1978).
- [7] I.Dunietz, H.Quinn, A.Snyder, W.Toki and H.J.Lipkin, Phys. Rev. D **43**, 2193 (1991).
- [8] K.Abe, M.Satpathy and H.Yamamoto, “Time-dependent angular analysis of B decays,” hep-ex/0103002 (2001).
- [9] K.Abe, *et al.* (Belle Collaboration) Phys Lett. **B538**, 11 (2002)
- [10] M.Suzuki, Phys. Rev. D **64**, 117503 (2001).
- [11] A.Datta and D.London, Int.J.Mod.Phys. **A19**,2505 (2004)
- [12] K.Abe *et al.* (Belle Collaboration) Phys. Rev. Lett. **88**, 171801 (2002).
- [13] S.Eidelman *et al.* (Particle Data Group), Phys. Lett. **B592**, 1 (2004).
- [14] Heavy Flavor Averaging Group, see “<http://www.slac.stanford.edu/xorg/hfag/>”.
- [15] M.Verderi, “Measurements Related to the CKM Angle β/ϕ_1 from BaBar,” hep-ex/0406082 (2004).
- [16] R.Itoh, “Measurements of time dependent CP asymmetry in $B \rightarrow VV$ decays with BELLE,” hep-ex/0210025 (2002).